Fuzzy Logic Controller-based Synchronverter in Grid-connected Solar Power System with Adaptive Damping Factor*

*Kah Yung Yap, Chee Ming Beh and Charles R. Sarimuthu**

(Department of Electrical and Computer Systems Engineering (ECSE), School of Engineering, Monash University Malaysia, Subang Jaya 47500, Malaysia)

Abstract: In recent years, renewable energy sources, specifically solar power systems, have developed rapidly owing to their technological maturity and cost effectiveness. However, its grid integration deteriorates frequency stability because of insufficient rotating masses and inertial response. Hence, a synchronverter, which is an inverter that mimics the operation of a synchronous generator, is crucial to interface solar power in a power grid. It stabilizes the power grid by emulating a virtual inertia. However, a conventional proportional-integral (PI)-based synchronverter is not equipped with an adaptive damping factor (D_p) or a digitalized smart controller to manage fast-responding solar inputs. Hence, a novel fuzzy logic controller (FLC) framework is proposed such that the synchronverter can operate in a grid-connected solar power system. In this study, D_p is controlled in real time using an FLC to achieve balance between speed and stability for frequency error correction based on frequency difference. Results of four case studies performed in Matlab/Simulink show that the proposed FLC-based synchronverter can stabilize the grid frequency by reducing the frequency deviation by at least 0.2 Hz (0.4%), as compared with the conventional PI-based synchronverter.

Keywords: Fuzzy logic controller (FLC), synchronverter, renewable energy system (RES), grid stability, solar power system

1 Introduction

The demand for global electricity has increased significantly in the past decade [1]. To fulfill electricity demand, many grid operators from different countries have transitioned toward renewable energy sources (RESs) [2] owing to their cost effectiveness and environmental friendliness [3]. Among RESs, solar power systems are popular because of their cost effectiveness [4], sustainability, and technological maturity [5]. As the power system evolves from centralized generation from oil and gas to distributed generation from RESs [6], the involvement of power-electronics-based converters is indispensable for ensuring power system stability [7-8]. Unlike the conventional synchronous machine (SM), solar inverters [9-10] in grid-connected solar power systems present disadvantages of zero inertial response, fast-changing behavior, and insufficient rotating masses [8]. The static structure of a converter deteriorates the frequency instability because of its inability to inject or absorb active power (P) from the rotating inertia based on the power demand [11]. If a sudden load change that causes power imbalance occurs [12], then the grid alternating current (AC) frequency will deviate from its nominal operating value [13]. This will affect the power supply quality and result in power supply discontinuity [14]. The current solution for controlling the solar power system is to inject the maximum power into the power grid [15]; however, this method is only suitable when solar power contributes insignificantly to the grid power capacity. Maximum power point tracking (MPPT) [16] can be performed to extract the maximum power from a solar array [17]; however, it does not contribute to the system inertia [18]. Such a problem can be mitigated using large-scale grid power. In addition to frequency regulation via active power (P), reactive power manipulation is performed to regulate the grid

Manuscript received April 30, 2020; revised May 5, 2020; accepted May 11, 2020. Date of publication June 30, 2021; date of current version June 4, 2021.

* Corresponding Author, E-mail: charles.raymond.sarimuthu@monash.edu

* Supported by the School of Engineering, Monash University Malaysia and Ministry of Higher Education (MoHE), Malaysia (FRGS/1/2019/TK07/MUSM/03/1).

Digital Object Identifier: 10.23919/CJEE.2021.000014

voltage [19] for the grid integration of RESs with low voltage ride through capability [20].

To alleviate the aforementioned problems, an inverter that mimics the inertial response of an SM must be used to integrate a solar power system with a power grid [21]. This type of inverter is known as a synchronverter or virtual synchronous generator [22], which is based on virtual inertia (VI) emulation [23]. A synchronverter can stabilize the operating frequency [24] when a sudden load change occurs by altering the electric torque (T) and active power (P). This emulated T is the synthetic inertia in the synchronverter. Research pertaining to synchronverter controllers has been performed in several areas, such as power frequency (p-f) control, direct-current (DC) link voltage controllers [25], self-synchronous controllers, damping correction loops [26], neural networks [27], and model predictive control [28].

However, research pertaining to digitalized fuzzy logic for synchronverter smart controllers is limited. Moreover, the damping factor (D_p) is fixed and cannot be adjusted based on the frequency deviation. To overcome the limitations of existing studies, a digitalized fuzzy logic controller (FLC) framework is proposed herein to control a synchronverter using an adaptive D_p. The core idea of the proposed FLC-based controller is to utilize the frequency difference (e) and rate of change of the frequency difference (de/dt) as inputs to fuzzy logic. Subsequently, a set of fuzzy rules is determined to control the D_p of the synchronverter. The adaptive value of D_p depends on the values of e and de/dt for balancing between transient recovery speed (lower D_p) and dampening stability (higher D_p). By controlling D_p, the operating frequency can resume to its nominal value even when sudden changes or faults occur. Four case studies were simulated in Matlab/Simulink, and the results are presented herein. The main contributions of this study are as follows.

(1) A novel digitalized FLC framework is designed for a synchronverter controller to stabilize the operating frequency of a grid-connected solar power system under sudden load changes.

(2) The D_p of the synchronverter is manipulated to be adaptive using an FLC to achieve balance between speed and stability based on the frequency deviation.

(3) The solar power system in a real-world environment with varying irradiance and temperature is considered for the design of the FLC framework.

The remainder of this paper is organized as follows. An overview of the synchronverter modeling is presented in Section 2. Section 3 describes the methodological setup of the FLC-based synchronverter in Matlab/Simulink. The simulation results from the four case studies are presented in Section 4. Finally, conclusions are provided in Section 5.

2 Modeling of synchronverter

In general, a synchronverter is defined as a power-electronics-based inverter that converts a DC to an AC while emulating the dynamic behaviors of a conventional synchronous generator (SG) [29]. A synchronverter comprises a conventional DC-AC inverter [30] that includes an inductor-capacitor (LC) filter, electronic switching devices, and an electronic pulse width modulation controller [31]. It is segregated into power (hardware) and electronic (controller) sections [32]. The power section converts DCs to ACs, whereas the electronic section is a measuring and control unit [33], which will be focused on herein.

As shown in Fig. 1, a synchronverter is used to interface the DC input from the solar panel with the power grid at the point of common coupling (PCC) [34], where V_{dc}, V_{abc}, V_m, and V^* represent the direct current voltage, three-phase voltage, measured feedback voltage, and reference voltage, respectively; L and L_g represent the inductor and grid inductance, respectively; P_e and P_t represent the electromagnetic power and mechanical power, respectively; C, i, E_o, f, and Q are the capacitor, current, generated output voltage reference, frequency, and reactive power, respectively.

The synchronverter exhibits the advantages and disadvantages of an SM. For example, loss stability due to oscillation around the synchronous frequency may occur in an SM and synchronverter. However, the parameters of a synchronverter, such as the moment of inertia (J), mutual inductance (L_M), field inductance (L_F), and D_p can be manipulated and

varied, unlike an SM. Fig. 2 shows the electronic section (controller) of a synchronverter, where J is the moment of inertia, $1/s$ is the integrator, P is the active power, Q is the reactive power, e is the generated reference voltage output, and V_m is the measured feedback voltage.

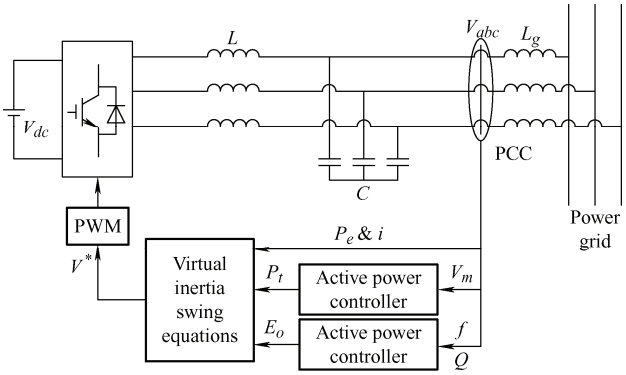

Fig. 1 Power section of synchronverter

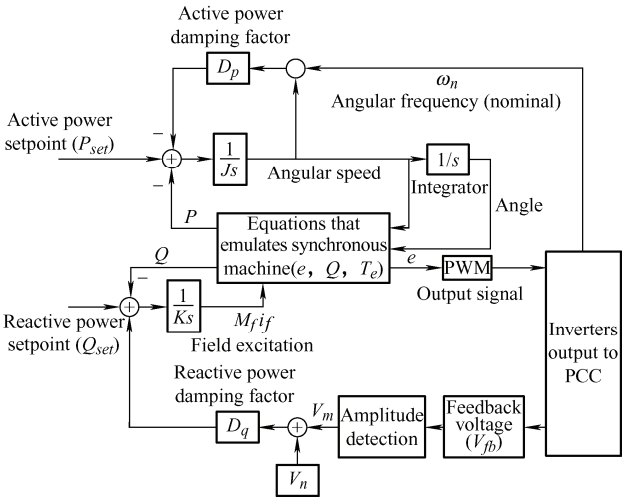

Fig. 2 Electronic section of synchronverter

Eqs. (1), (2), and (3) are used to model the SM for the controller of a synchronverter [35]. These equations mathematically describe the dynamics of an SM [36]. The power section of the synchronverter interacts with the controller using feedback measurement signals e and i.

$$T_e = M_f i_f < i, \widetilde{\sin\theta} > \tag{1}$$

$$Q = -\theta M_f i_f < i, \widetilde{\sin\theta} > \tag{2}$$

$$e = \dot{\theta} M_f i_f \widetilde{\sin\theta} \tag{3}$$

The controller of a synchronverter comprises an active power loop (APL) and a reactive power loop (RPL) [37]. The function of frequency droop control or APL is to control P when regulating the grid frequency (f_g), and the function of voltage droop control or RPL is to control Q when regulating the grid voltage. The rotor speed of the SG is maintained by the prime mover, and D_p arises from mechanical friction. When the demand for P increases, the electromagnetic torque increases as well, resulting in a decrease in speed. Consequently, the power regulation system will increase the mechanical power required to achieve a new power balance. This mechanism is known as frequency droop, which has been implemented in a synchronverter. Because the synchronverter does not have a prime mover (unlike an SM), this mechanism can only be achieved by comparing the virtual angular speed $\dot{\theta}$ and angular frequency reference $\dot{\theta}_r$ [38]. Based on the block, the effect of the frequency droop control loop is equivalent to a significant increase in D_p, which is the combination of an imaginary mechanical friction coefficient and the drooping frequency coefficient. The expression for D_p is shown in Eq. (4). By adding this mechanism, the synchronverter shares the load variation with other inverters automatically.

$$D_p = -\frac{\Delta T}{\Delta \theta} \tag{4}$$

Eqs. (5) and (6) express the rotor motion of the SG, where ω_N and ω are the nominal and actual values of the rotor angular speed, respectively; P_t and P_e represent the mechanical and electromagnetic powers of the synchronverter, respectively; J is the moment of inertia, and D is the damping ratio of the system.

$$\Delta\omega = \omega - \omega_N \tag{5}$$

$$J\frac{\mathrm{d}\omega}{\mathrm{d}t} = \frac{P_t - P_e}{\omega_N} - D\Delta\omega \tag{6}$$

When the system is grid connected, the frequency must be adjusted via governor control, as shown in Eq. (7).

$$P_t = P_N + \left(K_f + \frac{K_i}{s}\right)(\omega_N - \omega) \tag{7}$$

where P_N is the rated power of the synchronverter; K_f and K_i are the proportional gain and integral gain of the proportional-integral (PI) controller, respectively. Hence, the parameters that affect the response of the synchronverter controller are J and D_p. Instead of setting both parameters as fixed values, manipulating their values based on the frequency error tracking will

significantly improve the performance of the synchronverter controller.

3 FLC for synchronverter

In this section, the proposed FLC framework for the synchronverter in a grid-connected solar power system is discussed and presented.

3.1 Proposed FLC-based synchronverter

Fuzzy logic can be categorized as Mamdani and Sugeno types [39]. For the design of the FLC in this study, the Mamdani FLC with simple "if-then" relations were used [40]. Defuzzification based on the center-of-gravity technique was used for the FLC. To design an FLC for the synchronverter, the value of D_p was selected as the output of the FLC. It was used to balance the transient recovery speed and dampening stability of f_g. The frequency difference error ($e=f_n-f_g$), where f_n is the nominal frequency at 50 Hz and f_g is the grid frequency, as well as de/dt serve as the inputs of the fuzzy logic, as depicted in Fig. 3. These inputs are crucial for determining D_p, as the FLC must understand the frequency situation in real time.

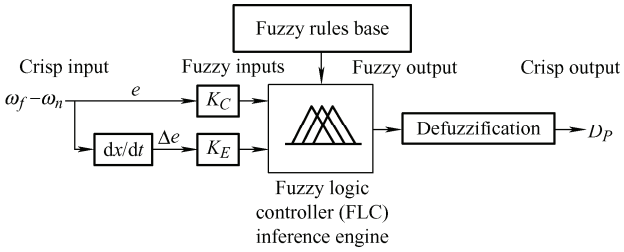

Fig. 3 Mamdani fuzzy inference engine

The value of D_p is high when both e and de/dt are high (positive or negative); similarly, the value of D_p is small when e and de/dt are small (positive or negative) or have zero errors. This is because when the frequency deviates significantly from its nominal value, a significant overshooting or frequency drop occurs owing to initialization or sudden load changes; hence, D_p should be sufficiently high to achieve an effective fast-responding dampening effect. By contrast, when the frequency deviation is small or negligible, stability is more important; hence, a lower value of D_p should be selected to smoothen the steady-state error. Figs. 4a-4c show member function plots of the frequency difference, rate of change of frequency, and D_p output, respectively.

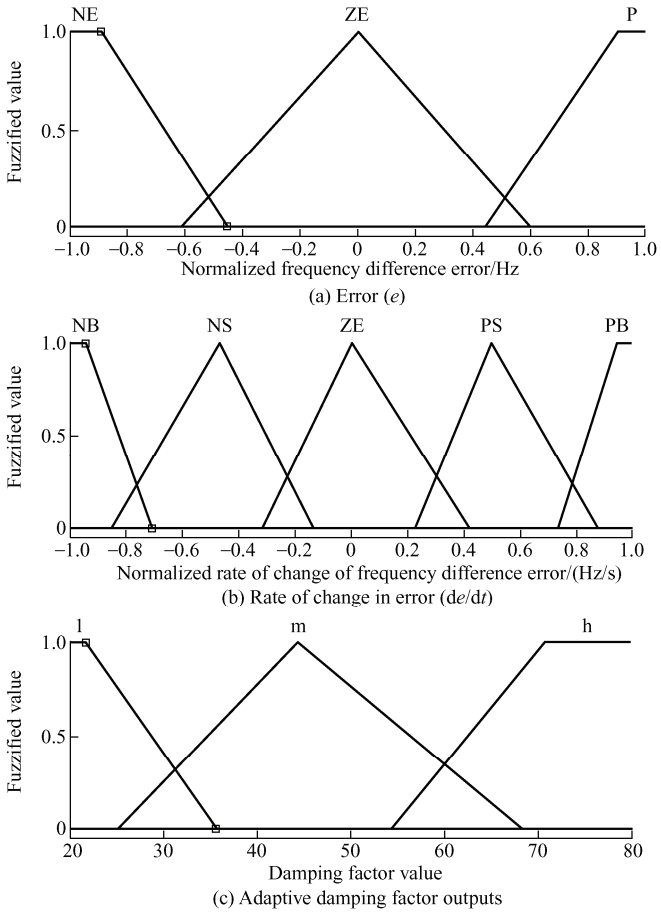

Fig. 4 Membership function of FLC

Tab. 1 shows the rule for the proposed FLC-based synchronverter. Input 1: e and input 2: de/dt determine the output values of D_p, where h, m, and l represent high (70 Nms/rad), intermediate (50 Nms/rad), and low (30 Nms/rad) values.

Tab. 1 Fuzzy rules used for proposed controller

Input 1: e	Input 2: de/dt				
	NB	NS	ZE	PS	PB
N	h	m	l	h	h
ZE	m	l	l	l	m
P	h	m	m	m	h

If e is negative, then the value of f_g is less than the f_n at 50 Hz. By contrast, a positive value of e implies that f_g is higher than f_n. If f_g continues to decrease, then de/dt will be negative. By contrast, a positive value of de/dt implies that f_g increases. When both e and de/dt show either high positive or negative values, f_g becomes unstable because of sudden load changes or faults. Consequently, the FLC will output a higher D_p such that the synchronverter can adjust the higher VI when dampening f_g. This is performed such that f_g can resume to its nominal value at 50 Hz rapidly

without stability issues. However, if e and de/dt have lower values, then D_p will be lower such that grid stability rather than recovery speed is emphasized. Fig. 5 and Fig. 6 illustrate the three-dimensional surface plot for the proposed FLC and the rule viewers of the implementation of the FLC, respectively.

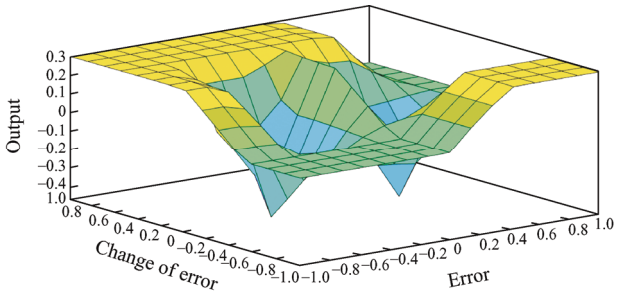

Fig. 5 Three-dimensional surface plot

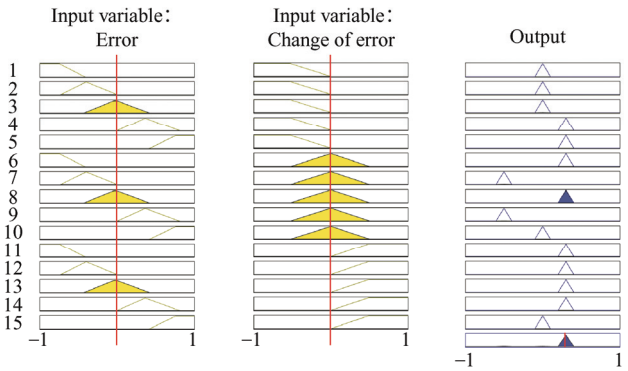

Fig. 6 The rules viewer of fuzzy logic controller

3.2 Modeling of FLC-based synchronverter controller in Matlab/Simulink

After designing the FLC framework in the built-in fuzzy logic toolbox, the model for the FLC-based synchronverter was developed in Matlab/Simulink. Using typical SM mathematical formulas, as stated in Section 2, the proposed FLC-based synchronverter model was built in a grid-connected solar power system. Fig. 7 depicts the controller block diagram of a synchronverter, which includes a p-f controller for the APL, a voltage regulator for the RPL, and a synchronverter equation block. This study focuses on APL for frequency regulation.

The APL controller uses the e of the system to simulate the mechanical power as a control input into the synchronverter block to emulate the VI, as illustrated in Fig. 8. Fig. 9 shows the rotor function block, which is a sub-block inside the synchronverter block. In this block, the inertia and damping factors are used to emulate the VI. The values of D_p are set as the nominal value before starting or initializing the system. After initializing the system, some of the error functions of the parameter can be determined, and D_p can be manipulated based on fuzzy rules.

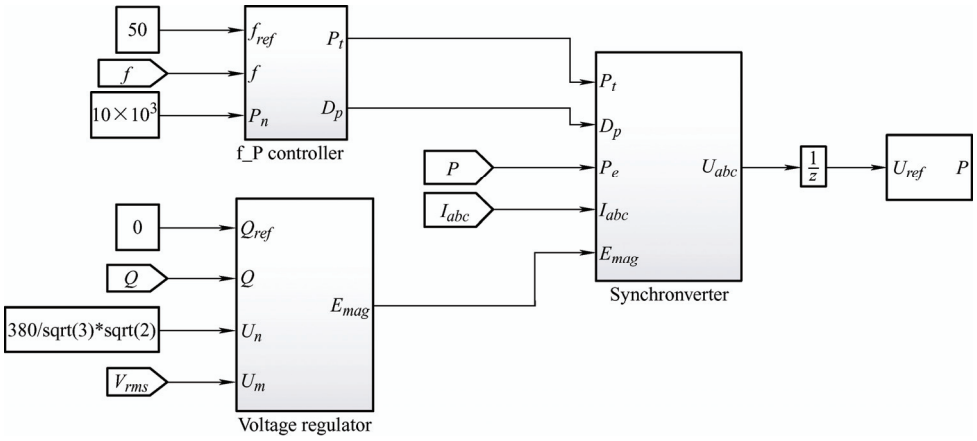

Fig. 7 FLC-based synchronverter controller

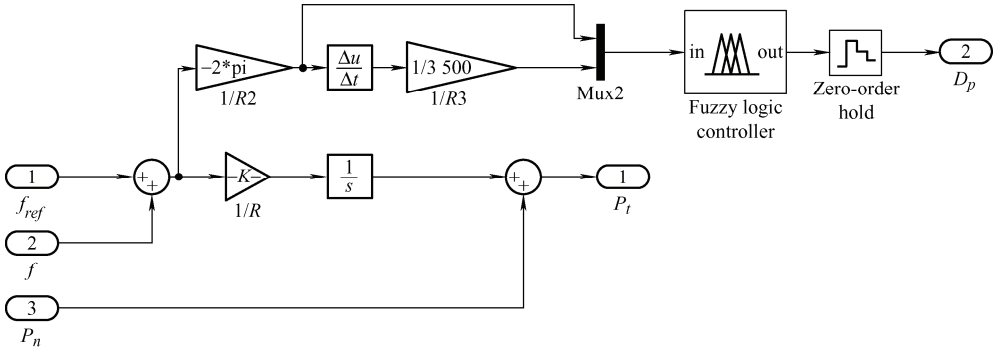

Fig. 8 The FLC-based framework in APL

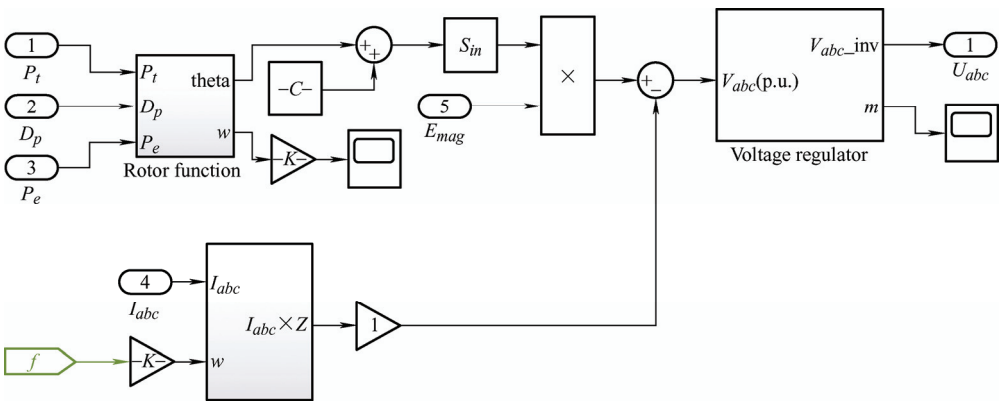

Fig. 9 Synchronverter internal block with rotor function

Tab. 2 presents the simulation parameters for the proposed synchronverter. D_p ranged from 30 to 70 Nms/rad (to be controlled by the FLC), and it was dependent on e and de/dt. The LC filter was used to filter the current and voltage ripples produced during the switching time.

Tab. 2 Parameters of proposed synchronverter

Parameter	Value
Rated DC voltage V_{DC}/V	100
AC phase voltage V_{AC}/kV	33
Nominal AC frequency f_n/Hz	50
Nominal AC angular speed ω_n/(rad/s)	314.16
Nominal resistive load R_L/kW	10
Moment of inertia J/(kg·m^2)	0.5
Adaptive damping factor D_p/(Nms/rad)	30-70
Frequency droop Δf	4% over 100% ΔP
Inverter power rating P_{RATED}/kW	10
Filter inductance L_f/mH	18.4
Filter capacitance C_f/μF	1
Line inductance L_{eq}/μH	1
Line resistance R_{eq}/mΩ	500
Time constant of APL τ_f/s	0.002

3.3 Testing environment in grid-connected solar power system

After designing the FLC controller and modeling the synchronverter, the proposed FLC-based synchronverter was simulated in a testing environment comprising a solar panel with varying irradiance and temperature, incremental-conductance-based MPPT, and a power grid at the PCC. Fig. 10 shows the overall simulation environment in Matlab/Simulink. The irradiance and temperature were varied to emulate a real-world environment with dynamic weather. The local resistive load was manipulated using a circuit breaker (CB) to emulate sudden load changes. Four test cases were considered to investigate the performance of the proposed FLC by varying the solar inputs and load changes, as shown in Tab. 3.

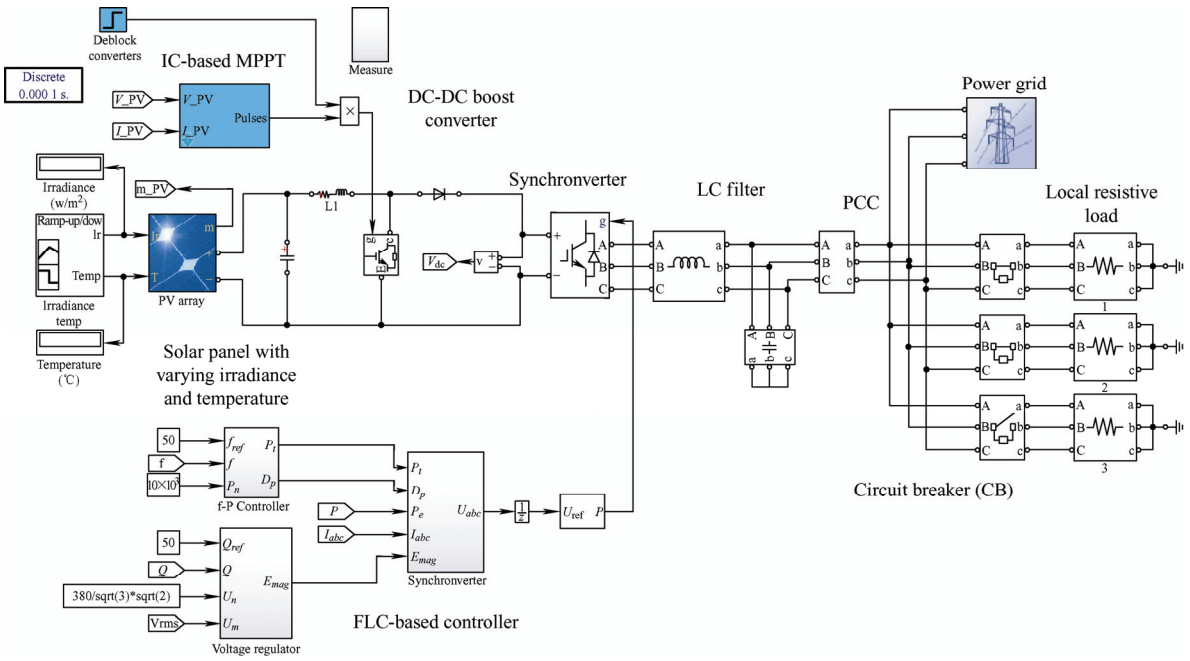

Fig. 10 Simulated solar panel with varying irradiance and temperature

Tab. 3 Variation for case studies

Case	Input	Load change
1	Constant ideal DC source	Yes
2	Solar panel with constant irradiance and temperature	Yes
3	Solar panel with varying irradiance and temperature	No
4	Solar panel with varying irradiance and temperature	Yes

To validate the effectiveness of the proposed FLC-based synchronverter, the solar inputs and load were varied for the case studies. The DC input side comprised either a constant DC input (ideal condition) or a solar panel input under dynamic weather. For the sudden load change, the resistive load was rated at 10 kW, which was then increased to 12 kW at $t = 0.5$ s and then decreased to 8 kW at $t = 1$ s. This was performed to investigate the frequency output performance of the proposed FLC-based synchronverter under sudden load changes. The simulation was conducted for 5 s. The performance indices of the FLC-based synchronverter were determined by two factors. First, the controller can execute frequency error correction, in which the frequency error will be controlled within ±1% (0.5 Hz) of the nominal value at 50 Hz. Second, the controller should be able to execute frequency error correction within a specific time range. Figs. 11a and 11b show the current-voltage *(I-V)* and power-voltage (*P-V)* characteristic curves of the solar panel (Model: SunPower SPR-305E-WHT-D), respectively.

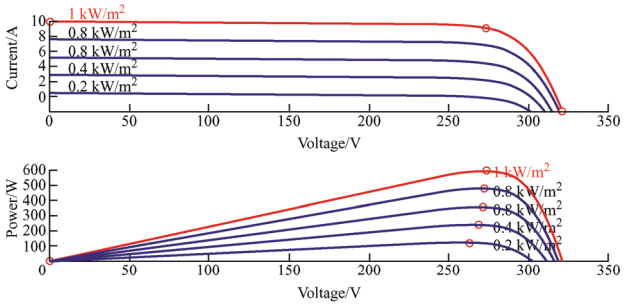

(a) *I-V* and *P-V* characteristic curves under varying solar irradiance

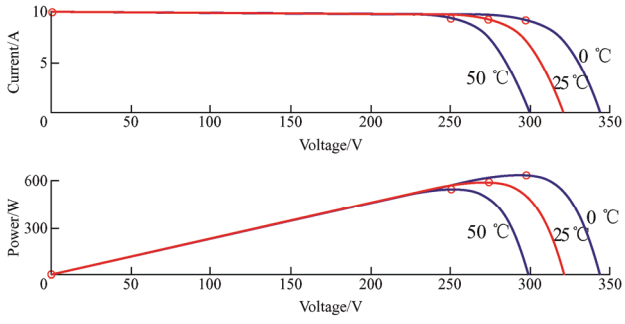

(b) *I-V* and *P-V* characteristic curves under varying operating temperatures

Fig. 11 *I-V* and *P-V* characteristics curves of solar array under varying input parameters

4 Simulation results and discussion

4.1 Constant DC input with sudden load change

In the first test case, the ideal constant DC input (battery) was used as the DC power source to investigate the performance of the synchronverter under a stable input. Fig. 12 shows the load change over time.

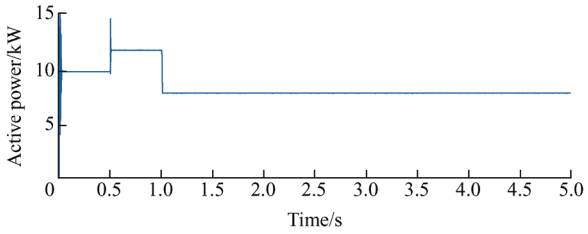

Fig. 12 Active power for varying resistive loads (R_L)

The resistive load (R_L) was rated at a nominal value of 10 kW. Using the CB block in Simulink, a sudden load increase was applied to the system at $t = 0.5$ s and the load side became 12 kW. Subsequently, a sudden load decrease was applied at $t = 1$ s and then decreased to 8 kW. The R_L remained at the same level for the remaining 4 s. Figs. 13a and 13b present plots of f_g and D_p.

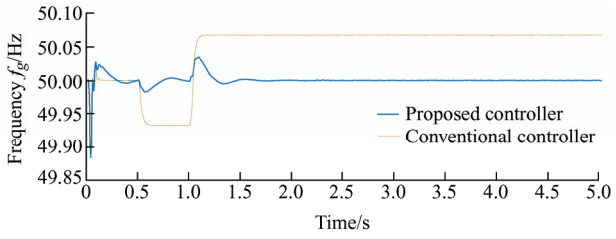

(a) Frequency grid (f_g) response at PCC

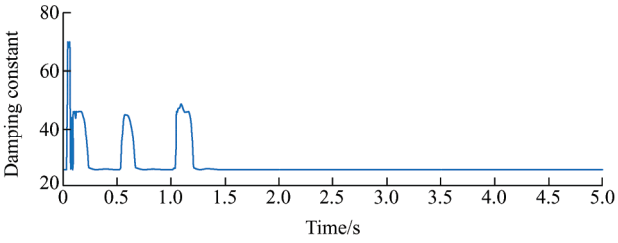

(b) Adaptive damping factor (D_p) of proposed controller

Fig. 13 Outputs of synchronverter for first case study

At $t = 0$ s, f_g decreased significantly owing to the initialization of the system. At this time, f_g deviated significantly from the f_n at 50 Hz. Hence, the FLC emulated a large D_p to dampen the decrease in frequency such that the transient of the decreasing frequency is reduced and the f_n value will be resumed after the completion of error correction by the FLC. At $t = 0.5$ s, a sudden load increase occurred when the CB with an additional R_L was closed; it was observed that

f_g decreased slightly below its rated value because power demand was greater than power generation. An imbalance in power delivery and consumption caused frequency disturbance. Therefore, the FLC immediately manipulated the adaptive damping constant to recover f_g to its nominal value. Similarly, at t = 1 s, a sudden load decrease occurred when the CB with an additional R_L was opened; the frequency of synchronverter was operated slightly above its rated value because power delivery exceeded power demand. In this opposing situation, the FLC instantly manipulated the damping constant to a higher value to recover f_g. The overall results validated the effectiveness of the synchronverter with FLC. The adaptive manipulatable D_p of the FLC framework performed better in terms of frequency recovery speed and stability compared with the conventional PI-based synchronverter controller under a constant DC source input and a sudden load change. The proposed FLC can complete the frequency error correction to its rated value at 50 Hz within 5 s. By contrast, the conventional synchronverter can only stabilize f_g at 50.07 Hz instead of at 50 Hz.

4.2 Solar panel input (constant irradiance and temperature) with sudden load change

In the second case study, we investigated the performance of the proposed FLC controller based on a real solar panel instead of a battery. As shown in Figs. 14a and 14b, two inputs were used, i.e., the solar irradiance and operating temperature, which were configured as a constant maximum at 1 000 W/m^2 and 50 ℃, respectively. Fig. 14c shows the P of the resistive load.

In this case study, a sudden load increase and decrease were applied at t=0.5 s and t=1 s, respectively. Figs. 15a and 15b show the simulation results under this test condition. It was observed that the f_g oscillated owing to the load changes; f_g indicated a significant overshooting within the first 3 s owing to system initialization.

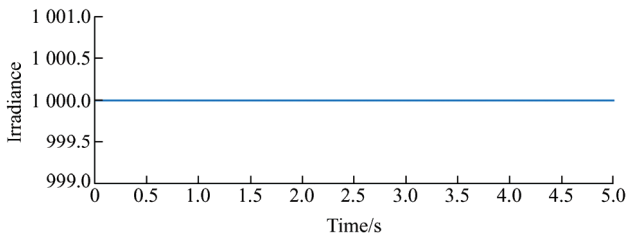

(a) Solar irradiancelevel of solar array

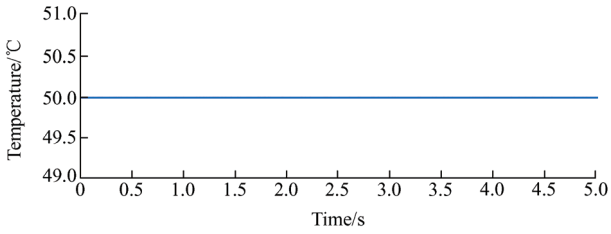

(b) Operating temperature level of solar array

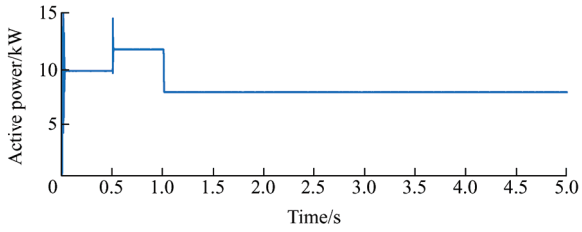

(c) Active power of varying resistive loads (R_L)

Fig. 14 Testing environment for second case study

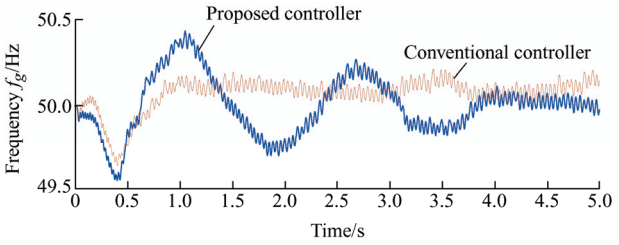

(a) Frequency response (f_g) at PCC

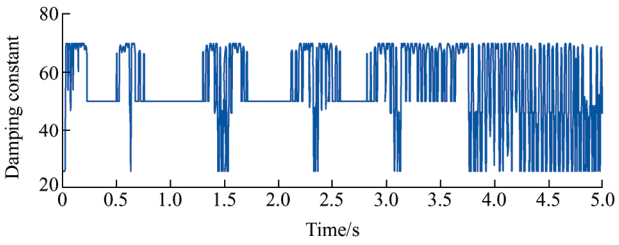

(b) Adaptive damping factor (D_p) of proposed controller

Fig. 15 Outputs of synchronverter for second case study

However, the proposed controller was able to stabilize f_g within a ±0.5% range after 3 s. The system simulated the different values of D_p based on the different conditions and fuzzy rules. The sudden load change only affected f_g by ± 0.1. In summary, the proposed FLC maintained f_g at approximately 50 Hz ± 0.1 Hz within 5 s. The conventional controller has a larger range of f_g oscillations of approximately ± 0.15. Although the proposed FLC controller exhibited a higher overshooting during the initialization, it demonstrated a better and more stable operating frequency after settling.

4.3 Solar panel input (varying irradiance and temperature) with constant load

In the third case study, the two inputs of the solar panel, i.e., irradiance and temperature, were

configured as ramp inputs with varying values. This was performed to investigate the performance of the proposed FLC-based synchronverter controller in a real-world environment with dynamic weather. The DC output of the solar panel depended significantly on the weather, particularly the irradiance and temperature. As depicted in Figs. 16a and 16b, both the irradiance and temperature were varied at different time frames to emulate the real weather. Meanwhile, R_L was set to 10 kΩ.

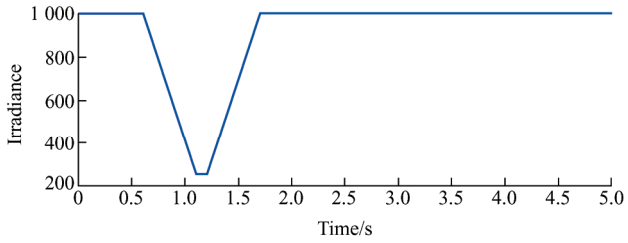

(a) Solar irradiance level of solar array

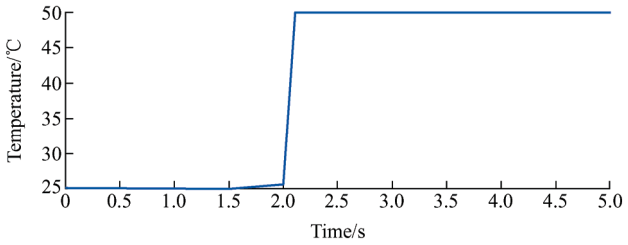

(b) Operating temperature level of solar array

Fig. 16 Testing environment for third case study

The irradiance value began at 1 000 W/m^2 and then slowly decreased at 0.6 s. It reached the value of 250 W/m^2 at 1.1 s and remained therein for approximately 0.1 s then increased again. It reached the value of 1 000 W/m^2 again at 1.7 s and remained therein until the end. Initially, the temperature was set to 25 ℃ for 2 s. After 2 s, the temperature was increased to 50 ℃until the end. Because no changes occurred at the load side, the focus of this case study was to investigate the effects of irradiance and temperature on grid stability. The proposed synchronverter controller can perform frequency error correction under dynamic weather conditions. Figs. 17a and 17b depict the frequency output and adaptive D_p, respectively. The frequency resulted in oscillation, which was caused by the instability of the solar panel as a power source under dynamic weather. The sudden decrease in solar irradiance at t = 1 s resulted in a decrease in f_g owing to an imbalance between power delivery and consumption.

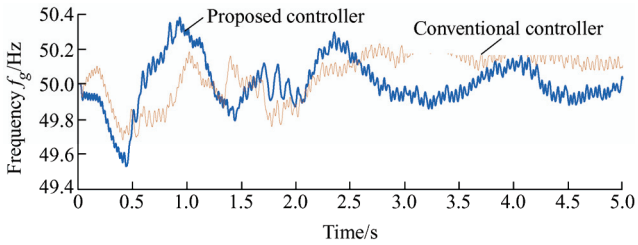

(a) Frequency response (f_g) at PCC

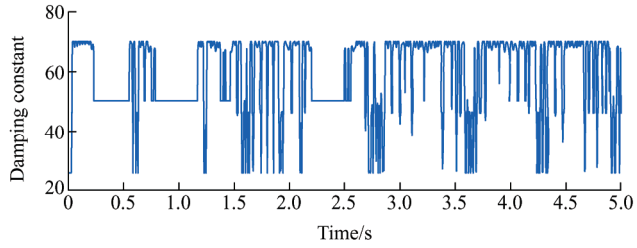

(b) Adaptive damping factor (D_p) of proposed controller

Fig. 17 Outputs of synchronverter for third case study

It was observed that a sudden increase in the operating temperature caused f_g to increase. This implies that the higher the input power, the higher is f_g because power generation exceeds power consumption. Based on the fuzzy rules configured in the FLC, the synchronverter selects and emulates the most optimal D_p value to control the VI-based synchronverter such that the frequency deviation can be corrected while balancing speed and stability, as shown in Fig. 17b. Although f_g exhibited a significant overshooting at the initialization time, the proposed FLC controller was able to dampen the overshooting frequency to its rated value at 50 Hz. The controller selected a higher value of D_p to dampen the overshooting at a faster rate than the conventional controller. The proposed controller performed error correction with high accuracy. The conventional controller can only limit f_g within a certain range and does not enable f_g to be resumed to the rated value. This can be easily verified by observing the simulation graph. The proposed controller was able to maintain a f_g of approximately 50 Hz with ± 0.1% error within 5 s. The conventional controller oscillated at approximately 50.1 Hz. Hence, the proposed FLC-based synchronverter controller enabled a better quality f_g to be obtained.

4.4 Solar panel input (varying irradiance and temperature) with sudden load change

In the fourth case study, a sudden load change was applied at the PCC, in addition to the varying

solar irradiance and temperature. Hence, it is important to prove that the proposed controller performs well. In this scenario, a controller that can provide a good function is the basic requirement. Fig. 18 show the testing conditions for the fourth case study.

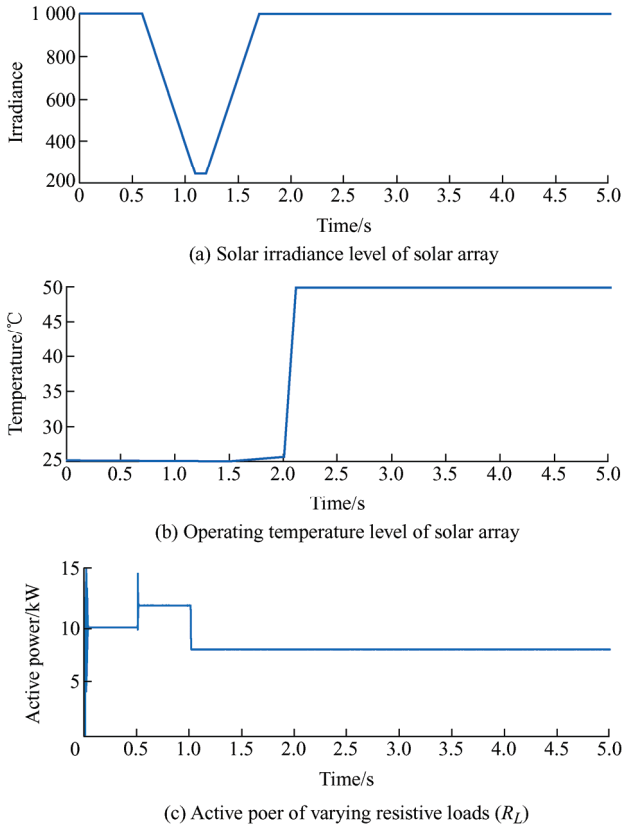

(a) Solar irradiance level of solar array

(b) Operating temperature level of solar array

(c) Active poer of varying resistive loads (R_L)

Fig. 18 Testing environment for fourth case study

In this particular case study, the values of varying irradiance and temperature were similar to those in the third case study. The only difference was the sudden load change that occurred at t=0.5 s (load increase) and t=1 s (load decrease) to investigate the performance of the proposed FLC controller when instabilities occurred at both the DC source and R_L sides. The sudden load change was manipulated using the three-phase CB model in Simulink for automatic load switching. At t=0.5 s, a CB is switched on to increase the R_L to 12 kW. At t=1 s, another CB was switched off to decrease the load to 8 kW. Fig. 19 show the simulation results. The actions above are analogous to electricity consumers turning on and off their equipment or machines at different time frames. By emulating sudden load changes and dynamic weather for solar panels, the synchronverter controller can perform optimally in the most demanding situations that may occur in real life.

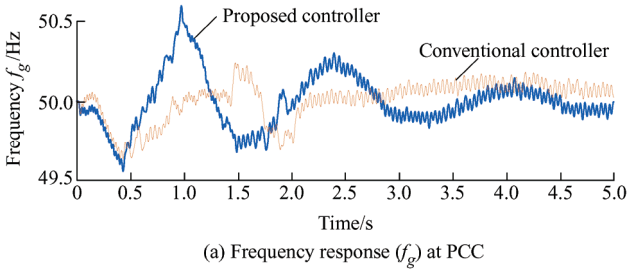

(a) Frequency response (f_g) at PCC

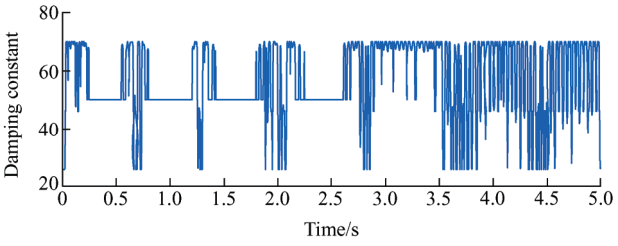

(b) Adaptive damping factor (D_p) of proposed controller

Fig. 19 Outputs of synchronverter for fourth case study

The result indicates that f_g exhibited a significant overshooting at t=1 s owing to a decrease in solar irradiance and a sudden load increase. Under this condition, the proposed FLC-based synchronverter can perform frequency error correction within 5 s. The f_g was controlled in the range of ± 0.1. In the first 2 s, f_g was highly unstable and exhibited significant overshooting. The system began to stabilize slowly after t=2.5 s, and the overshooting subsided. This case study proved that the performance of the proposed FLC controller was satisfactory under sudden load changes and dynamic weather conditions. The proposed FLC controller can perform a fast frequency error correction. By contrast, the conventional controller can only maintain f_g at a certain value after a disturbance and cannot perform fast frequency error corrections.

5 Conclusions

Herein, a novel FLC-based framework was proposed to control a synchronverter in a grid-connected solar power system under dynamic weather conditions. Four case studies were simulated in Matlab/Simulink, and the results validated the ability of the proposed controller in stabilizing f_g by reducing the frequency deviation by at least 0.2 Hz (0.4%), as compared with the conventional PI-based synchronverter. The performance of the FLC-based synchronverter was optimal even under sudden load

changes or varying irradiances and temperatures. P was injected or absorbed whenever the frequency decreased or increased, respectively. The D_p controlled by the FLC was able to balance between transient speed and stability, whereby a larger D_p afforded a more prominent dampening effect, and vice versa.

References

[1] H Zsiborács, N H Baranyai, A Vincze, et al. Intermittent renewable energy sources: The role of energy storage in the European Power System of 2040. *MDPI Electronics*, 2019, 8(7): 729.

[2] M Z Saleheen, A A Salema, S M M Islam, et al. A target-oriented performance assessment and model development of a grid-connected solar PV (GCPV) system for a commercial building in Malaysia. *Renewable Energy*, 2021, 171: 371-382.

[3] Y Wang, V Silva, A Winckels. Impact of high penetration of wind and PV generation on frequency dynamics in the continental Europe interconnected system. *IET Renewable Power Generation*, 2014, 10(1): 10-16.

[4] F Li, C Li, K Sun, et al. Capacity configuration of hybrid CSP/PV plant for economical application of solar energy. *Chinese Journal of Electrical Engineering*, 2020, 6(2): 19-29.

[5] G Perveen, M Rizwan, N Goel. Comparison of intelligent modelling techniques for forecasting solar energy and its application in solar PV based energy system. *IET Energy Systems Integration*, 2019, 1(1): 34-51.

[6] G I Rashed, H Haider, M B Shafik. Enhancing energy utilization efficiency of Pakistani system considering FACTS devices and distributed generation: Feasibility study. *Chinese Journal of Electrical Engineering*, 2020, 6(2): 66-82.

[7] P Anand, M Rizwan, S K Bath. Sizing of renewable energy based hybrid system for rural electrification using grey wolf optimisation approach. *IET Energy Systems Integration*, 2019, 1(3): 158-172.

[8] Z A Obaid, L M Cipcigan, L Abrahim, et al. Frequency control of future power systems: Reviewing and evaluating challenges and new control methods. *Journal of Modern Power Systems and Clean Energy*, 2019, 1(7): 9-25.

[9] E Lorenzani, G Migliazza, F Immovilli, et al. CSI and CSI7 current source inverters for modular transformerless PV inverters. *Chinese Journal of Electrical Engineering*, 2019, 5(2): 32-42.

[10] L Zhang, F Jiang, D Xu, et al. Two-stage transformerless dual-buck PV grid-connected inverters with high efficiency. *Chinese Journal of Electrical Engineering*, 2018, 4(2): 36-42.

[11] D Chen, Y Xu, A Q Huang. Integration of DC microgrids as virtual synchronous machines into the AC grid. *IEEE Transactions on Industrial Electronics*, 2017, 64(9): 7455-7466.

[12] K N Mude, K Aditya. Comprehensive review and analysis of two-element resonant compensation topologies for wireless inductive power transfer systems. *Chinese Journal of Electrical Engineering*, 2019, 5(2): 14-31.

[13] J K Reed, Q C Zhong, J Saniie. Digital synchronverter design flow for renewable energy. *IEEE International Conference on Electro Information Technology (EIT)*, May 14-17, 2017, Lincoln, NE, USA, IEEE, 2017: 363-366.

[14] J Roldán-Pérez, A Rodríguez-Cabero, M Prodanovic. Parallel current-controlled synchronverters for voltage and frequency regulation in weak grids. *The Journal of Engineering*, 2019, 17: 3516-3520.

[15] X Zhang, Q Gao, Y Hu, et al. Active power reserve photovoltaic virtual synchronization control technology. *Chinese Journal of Electrical Engineering*, 2020, 6(2): 1-6.

[16] A Ibrahim, M Shafik, M Ding, et al. PV maximum power-point tracking using modified particle swarm optimization under partial shading conditions. *Chinese Journal of Electrical Engineering*, 2020, 6(4): 106-121.

[17] K Y Yap, H S Chua, M J K Bashir, et al. Central composite design (CCD) for parameters optimization of maximum power point tracking (MPPT) by response surface methodology (RSM). *Journal of Mechanic of Continua and Mathematical Sciences (JMCMS)*, 2019, 1(1): 259-270.

[18] K Y Yap, C R Sarimuthu, J M Y Lim. Artificial intelligence based MPPT techniques for solar power system: A review. *Journal of Modern Power Systems and Clean Energy (MPCE)*, 2020, 8(6): 1043-1059.

[19] S Zheng, Z Li, M Cao. Direct current control strategy of SVG based on dual sequence dq coordinates under asymmetric load condition. *Chinese Journal of Electrical Engineering*, 2019, 5(1): 24-35.

[20] E Gatavi, A Hellany, M Nagrial, et al. An integrated reactive power control strategy for improving low voltage ride-through capability. *Chinese Journal of Electrical Engineering*, 2019, 5(4): 1-14.

[21] Q C Zhong, G C Konstantopoulos, B Ren, et al. Improved synchronverters with bounded frequency and voltage for smart grid integration. *IEEE Transactions on Smart Grid*, 2018, 9(2): 786-796.

[22] X Zhang, F Mao, H Xu, et al. An optimal coordination control strategy of micro-grid inverter and energy storage based on variable virtual inertia and damping of VSG. *Chinese Journal of Electrical Engineering*, 2017, 3(3): 25-33.

[23] T Younis, M Ismeil, M Orabi, et al. A single-phase self-synchronized synchronverter with bounded droop characteristics. *IEEE Applied Power Electronics Conference and Exposition (APEC)*, March 4-8, 2018, San Antonio, TX, USA, IEEE, 2018: 1624-1629.

[24] K Y Yap, C R Sarimuthu, J M Y Lim. Virtual inertia-based inverters for mitigating frequency instability in grid-connected renewable energy system: A review. *Applied Science (MDPI)*, 2019, 9(24): 5300.

[25] D Remon, A M Cantarellas, E Rakhshani, et al. An active power synchronization control loop for grid-connected converters. *IEEE PES General Meeting | Conference & Exposition*, July 27-31, 2014, National Harbor, MD, USA: 1-5.

[26] S Saadatmand, M S Sanjarinia, P Shamsi, et al. Dual heuristic dynamic programing control of grid-connected synchronverters. *North American Power Symposium (NAPS)*, Oct 13-15, 2019, Wichita, KS, USA.

[27] S Dong, Y C Chen. Adjusting synchronverter dynamic response speed via damping correction loop. *IEEE Transactions on Energy Conversion*, 2017, 32(2): 608-619.

[28] T Kerdphol, F S Rahman, Y Mitani, et al. Virtual inertia control-based model predictive control for microgrid frequency stabilization considering high renewable energy integration. *Sustainability*, 2017, 9(5): 773.

[29] R V Ferreira, S M Silva, H M A Antunes, et al. Dynamic analysis of grid-connected droop-controlled converters and synchronverters. *Journal of Control, Automation and Electrical Systems*, 2019, 30(5): 741-753.

[30] Y Zhang, J Xiong, P He, et al. Review of power decoupling methods for micro-inverters used in PV systems. *Chinese Journal of Electrical Engineering*, 2018, 4(4): 26-32.

[31] Q C Zhong, G Weiss. Synchronverters: Inverters That mimic synchronous generators. *IEEE Transactions on Industrial Electronics*, 2011, 58(4): 1259-1267.

[32] Q C Zhong, P L Nguyen, Z Ma, et al. Self-synchronized synchronverters: Inverters without a dedicated synchronization unit. *IEEE Transactions on Power Electronics*, 2014, 29(2): 617 - 630.

[33] R Aouini, I Nefzi, K B Kilani, et al. Exploitation of synchronverter control to improve the integration of renewable sources to the grid. *Journal of Electrical System*, 2017, 13: 543-557.

[34] S Dong, Y C Chen. A method to directly compute synchronverter parameters for desired dynamic response. *IEEE Transactions on Energy Conversion*, 2018, 33(2): 814-825.

[35] K Y Yap, C R Sarimuthu, J M Y Lim. Grid integration of solar photovoltaic system using machine learning-based virtual inertia synthetization in synchronverter. *IEEE Access*, 2020, 8: 49961-49976.

[36] L Shang, J Hu, X Yuan, et al. Improved virtual synchronous control for grid-connected VSCs under grid voltage unbalanced conditions. *Journal of Modern Power Systems and Clean Energy*, 2019, 7(1): 174-185.

[37] M J Y Liaw, C R Sarimuthu. Development of a synchronverter for a grid connected photovoltaic system. *IOP Conference Series: Materials Science and Engineering, Volume 767, 1st International Symposium on Engineering and Technology (ISETech)*, Feb. 1, 2019, Perlis, Malaysia: 2019, 767(1): 012046.

[38] D Sun, H Liu, S Gao, et al. Comparison of different virtual inertia control methods for inverter-based generators. *Journal of Modern Power Systems and Clean Energy*, 2020, 8(4): 768-777.

[39] C R Sarimuthu, V K Ramachandaramurthy, H Mokhlis, et al. Comparison of Mamdani-type and Sugeno-type fuzzy inference systems for transformer tap changing system. *International Journal of Advances in Applied Sciences*, 2016, 5(4): 163.

[40] H Mokhlis, K R Agileswari, C R Sarimuthu, et al. FLC based AVC relay with Newton Raphson load flow for voltage control in distribution network. *International Journal of Control Theory and Applications*, 2017, 10(16): 257-265.

Kah Yung Yap received the B. E. degree (Hons.) in electrical and electronic engineering from UCSI University, Malaysia. He is currently pursuing the Ph.D. degree in electrical and computer systems engineering (ECSE) with Monash University, Malaysia under Graduate Research Merit Full Scholarship. He is a graduate engineer of the Board of Engineers Malaysia (BEM) and a graduate member of the Institution of Engineers Malaysia (IEM). He is also a graduate student member of The Institute of Electrical and Electronics Engineers (IEEE), a society member in IEEE Power & Energy Society (PES) and a member of The Institution of Engineering and Technology (MIET). His current research interests include adaptive synchronverters, grid-connected solar power systems, and power quality improvement. He was awarded the 2017 IEM Gold Award Medal for the Best Engineering Student.

Chee Ming Beh currently is a final year Electrical and Computer Systems Engineering (ECSE) student in Monash University, Malaysia. His final year project (FYP) entitled "A new control framework for enhancing grid stability using synchronverters" focuses on the design of fuzzy logic controller for a synchronverter in grid-connected solar power system. His current research interests include grid-connected solar power system, synchronverter and fuzzy logic control framework.

Charles R. Sarimuthu received the B.E. and M.E. degrees in electrical engineering from the University of Malaya, Malaysia, in 2006 and 2010, respectively, and the Ph.D. degree in electrical power engineering from National Energy University, Malaysia, in 2019. He is a member of the Institution of Engineers Malaysia (IEM) and a registered engineer of the Board of Engineers Malaysia (BEM). In 2018, he joined as a Lecturer with the Department of Electrical and Computer Systems Engineering, School of Engineering, Monash University, Malaysia. His research interests include power systems, power quality, renewable energy, and smart grids.